Supporting Information

Preparations:

General Procedures and Materials: All chemicals and solvents in the synthesis were reagent grade and used as received. $Cs_3Mo(CN)_8 \cdot 2H_2O$ was prepared according to the literature.[s1] Perchlorate salt of metal compounds with organic ligand is potentially explosive and cyanides are toxic. These materials should be handled with great caution.

Caution: Perchlorate salt of metal compounds with organic ligand is potentially explosine. Only small amounts of material should be cautiously handled.

$\{Cd[HC(3,5\text{-}Me_2pz)_3]_2\}(NO_3)_2$: This was synthesized according to a modified procedure.[s2] $Cd(NO_3)_2 \cdot 6H_2O$ (0.1 mmol) was added to a THF (20 ml) solution of $HC(3,5\text{-}Me_2pz)_3$ (0.2 mmol). After the solution was stirred for 1 day, the resulting mixture was diffused with ether (150 ml) for 1 day. The white powders which had formed were filtered off, washed with ether, and dried in air. Yield: 52%. Anal. Calcd for $C_{32}H_{44}N_{14}O_6Cd$: C, 46.13; H, 5.32; N, 23.54. Found: C, 45.94; H, 5.55; N, 23.89.

$[Mo(CN)_8Mn(5\text{-}Brsalcy)]\{M[HC(3,5\text{-}Me_2pz)_3]_2\}\cdot x$(solvents) [M = Fe (1·2MeOH·5H_2O) and Cd (2·H_2O)]: $Cs_3Mo(CN)_8 \cdot 2H_2O$ (0.05 mmol) and $\{Fe[HC(3,5\text{-}Me_2pz)_3]_2\}(BF_4)_2$ (0.05 mmol) were added to a solution of $[Mn(5\text{-}Brsalcy)(H_2O)]ClO_4$ (0.05 mmol) in a mixed MeOH/acetone/H_2O solvent (5:5:1, v/v). After stirring for 1 min, the reaction solution was filtered and slowly evaporated in the dark at room temperature for 2 days. The red crystals (**1**) that had formed were filtered off, washed with MeOH/acetone and dried in air. Yield: 46%. The Cd analogue (**2**) was prepared with the same procedure except for using $\{Cd[HC(3,5\text{-}Me_2pz)_3]_2\}(NO_3)_2$ instead of $\{Fe[HC(3,5\text{-}Me_2pz)_3]_2\}(BF_4)_2$ and the yield is 27%. Anal. Calcd for $C_{62}H_{80}Br_2FeMnMoN_{22}O_9$: C, 45.30; H, 4.90; N, 18.76. Found: C, 45.05; H, 4.55; N, 18.90. Anal. Calcd for $C_{60}H_{64}Br_2N_{22}O_3MnCdMo$: C, 46.07; H, 4.12; N, 19.70. Found: C, 46.48; H, 4.15; N, 19.79.

(s1) L. D. C. Bok, J. G. Leipoldt, S. S. Basson, Z. *Anorg. Allg. Chem.*, 1975, **415**, 81.
(s2) D. L. Reger, C. A. Little, *Inorg. Chem.*, 2001, **40**, 1508.

Physical Measurements:

Elemental analyses for C, H, and N were performed at the Elemental Analysis Service Center of Sogang University. Infrared spectra were obtained from KBr pellets with a Bomen MB-104 spectrometer. Magnetic susceptibilities for **1** and **2** were carried out using a Quantum Design SQUID susceptometer (dc) and a PPMS magnetometer (ac). Diamagnetic corrections of all samples were estimated from Pascal's Tables. The pressure effect of the magnetic properties were carried out on an Easy-Lab Mcell 10 hydrostatic pressure cell which was designed for the MPMS set up with the silicone oil as pressure transmitting medium. The pressure was applied externally to the sample and measured by the pressure dependence of the superconducting transition temperature of a build-in pressure sensor made of high-purity tin. Magnetic data were calibrated for the sample holder and diamagnetism estimated from Pascal's constants.

Crystallographic Structure Determination:

X-ray data for **1** and **2** were collected on a Bruker SMART APEXII diffractometer equipped with graphite monochromated MoKα radiation (λ = 0.71073 Å). Preliminary orientation matrix and cell parameters were determined from three sets of ω scans at different starting angles. Data frames were obtained at scan intervals of 0.5° with an exposure time of 10 s per frame. The reflection data were corrected for Lorentz and polarization factors. Absorption corrections were carried out using SADABS. The structures were solved by direct methods and refined by full-matrix least-squares analysis using anisotropic thermal parameters for non-hydrogen atoms with the SHELXTL program. All hydrogen atoms except for hydrogen bound to water molecules were calculated at idealized positions and refined with the riding models. To check the space groups for **1** and **2**, ADDSYM/PLATON, an Algorithm for missing symmetry, was conducted and no obvious space group change was suggested. Crystal data of **1**·2MeOH·5H_2O: Mr = 1644.03, triclinic, space group *P*-1, *a* = 10.7696(6) Å, *b* = 13.8437(7) Å, *c* = 24.4199(14) Å, α = 89.154(3)°, β = 89.071(3)°, γ = 84.376(3)°, *V* = 3622.5(3) $Å^3$, *Z* = 2, D_{calc} = 1.507 g cm^{-3}, μ = 1.711 mm^{-1}, *T* = 90(2) K, 80068 reflections collected, 14300 unique (R_{int} = 0.0829), *R*1 = 0.0551, *wR*2 = 0.1303 [$I > 2\sigma(I)$]. Crystal data of **2**·2MeOH·5H_2O: Mr = 1700.58, triclinic, space group P-1, *a* = 10.7993(9) Å, *b* = 14.0068(11) Å, *c* = 24.4363(19) Å, α = 90°, β = 90°, γ = 94.227(4)°, V = 3686.3(5) $Å^3$, *Z* = 2, D_{calc} = 1.532 g cm^{-3}, μ = 1.773 mm^{-1}, *T* = 100(2) K, 19854 reflections collected, 13447 unique (R_{int} = 0.0556), *R*1 = 0.0850, *wR*2 = 0.2014 [$I > 2\sigma(I)$].

Table S1. Results of the continuous shape measure analysis.

Complex	Metal center	Shape Measures(S_X) relative to			Δ	φ	
		SAPR	DD	BTP	(SAPR, DD)	(SAPR> DD)	(DD> SAPR)
1	Mo1	2.80142	0.43270	2.46871	0.380	99.2%	38.8%
2	Mo1	2.21950	0.37973	2.82551	0.245	88.2%	36.4%

S_{DD} is the shape measure relative to the dodecahedron, S_{SAPR} the shape measure relative to the square antiprism, S_{BTP} the shape measure relative to the bicapped trigonal prism, Δ(SAPR,DD) indicates the deviation from the DD-SAPR interconversion path, and φ(SAPR>DD) and φ(DD>SAPR) the generalized interconversion coordinates. The sum φ(SAPR>DD) + φ(DD>SAPR) is larger than 100% because of the nonzero value of Δ(SAPR,DD). To determine the exact geometry around Mo we performed a continuous shape measures (CShM) analysis (Table S1). The S_X (X = SAPR, DD, BTP) values against ideal symmetry of a square antiprism (SAPR, D_{4d}), a dodecahedron (DD, D_{2d}), and a bicapped trigonal prism (BTP, C_{2v}) definitely disclose that the Mo ion is described as a distorted DD.

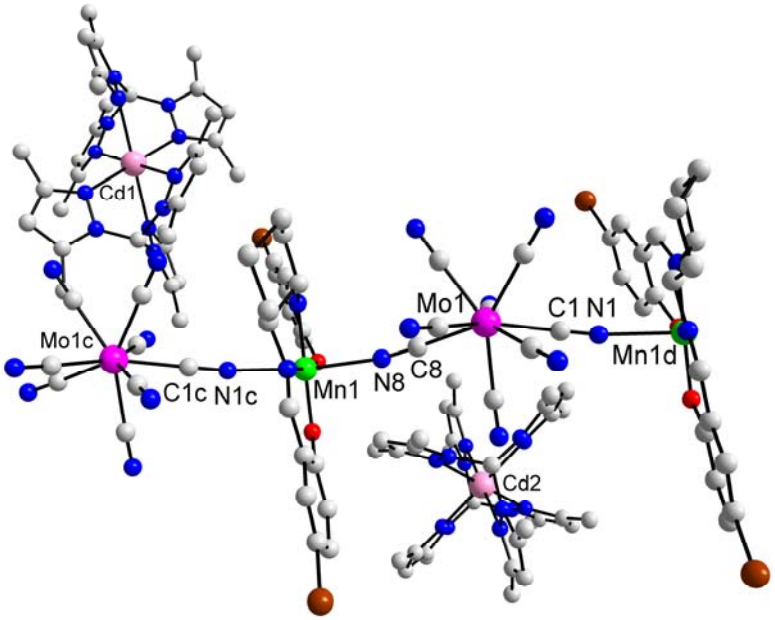

Fig. S1. Molecular view of **2**. Symmetry transformations used to generate equivalent atoms: c = -1+x, y, z and d = 1+x, y, z.

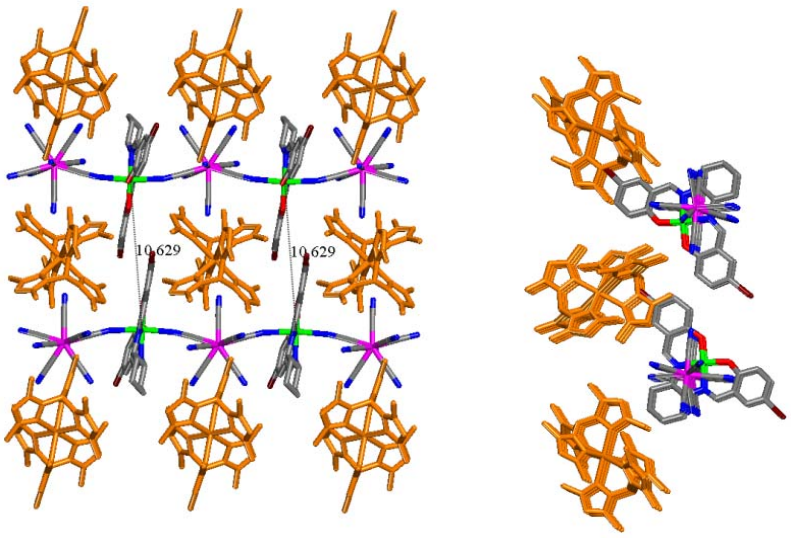

(a) (b)

Fig. S2. Extended view of **1** in the *ac* plane (a) and in the *bc* plane (b). The dotted lines represent the shortest distance between neighboring chains. The orange color represents Fe moieties in the crystal packing diagram.

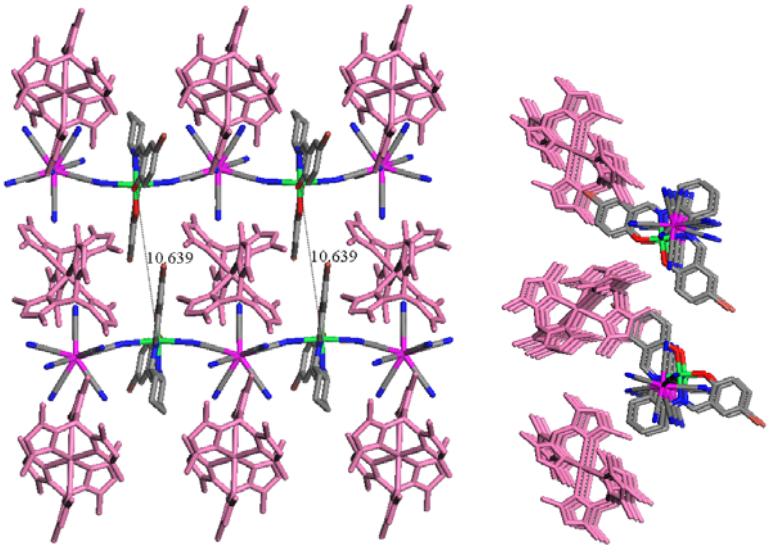

(a) (b)

Fig. S3. Extended view of **2** in the *ac* plane (a) and in the *bc* plane (b). The dotted lines represent the shortest distance between neighboring chains. The rose color represents Cd moieties in the crystal packing diagram.

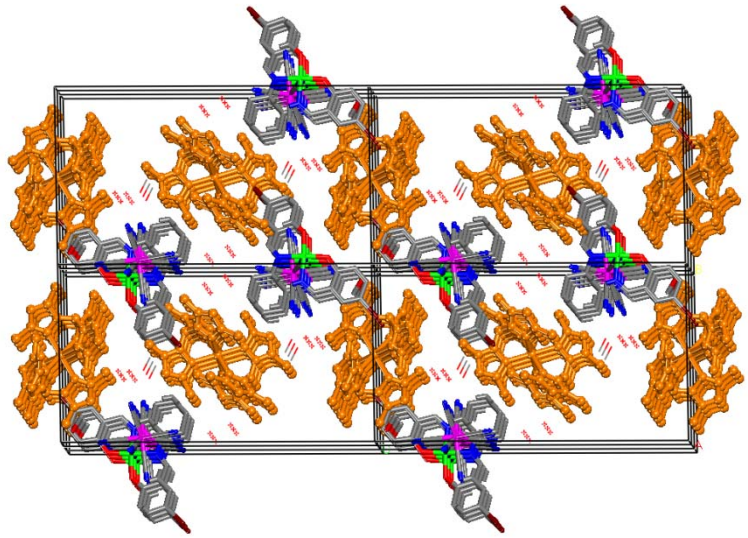

(a)

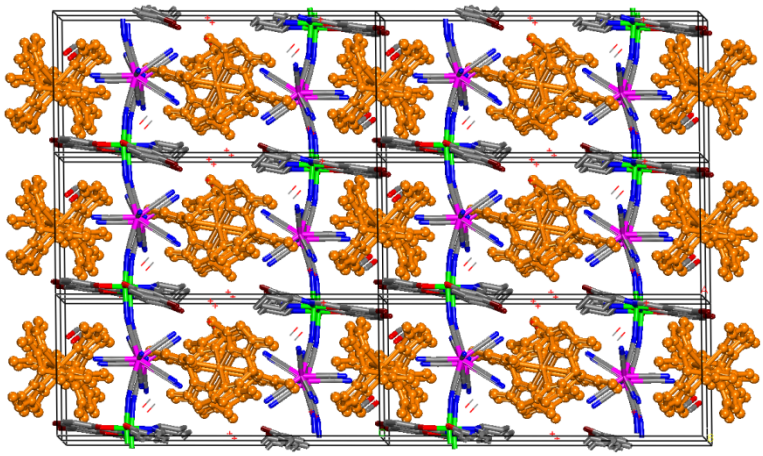

(b)

Fig. S4. Extended view of **1**. The 3D structures are shown in *bc* plane (a) and in the *ac* plane (b). The orange color represents Fe moieties in the crystal packing diagram.

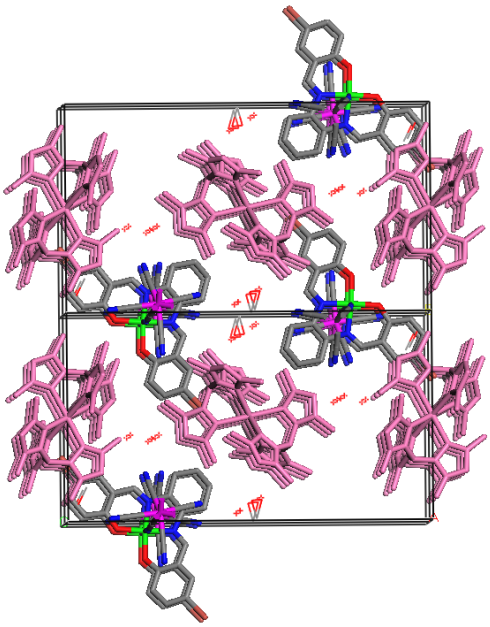

(a)

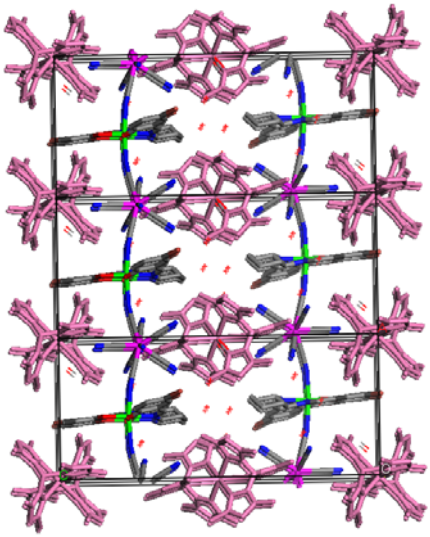

(b)

Fig. S5. Extended view of **2**. The 3D structures are shown in *bc* plane (a) and in the *ac* plane (b). The rose color represents Cd moieties in the crystal packing diagram.

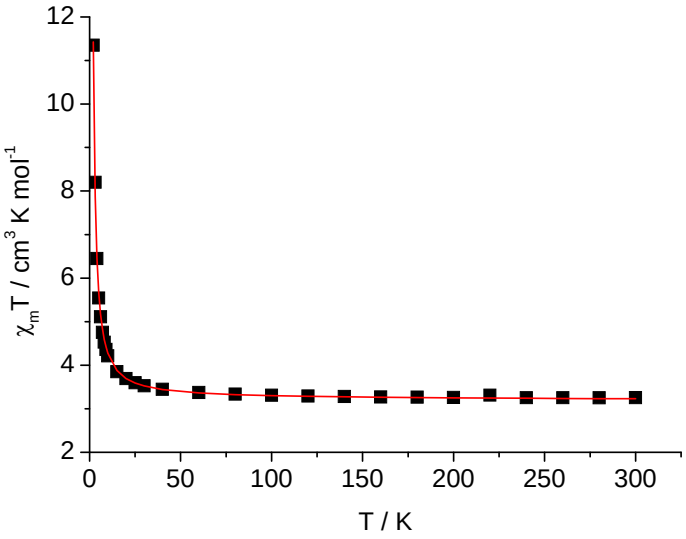

Fig. S6. Plot of $\chi_m T$ versus T at 1000 G for **2**. The solid line is a best fit of the data with the Seiden chain model.

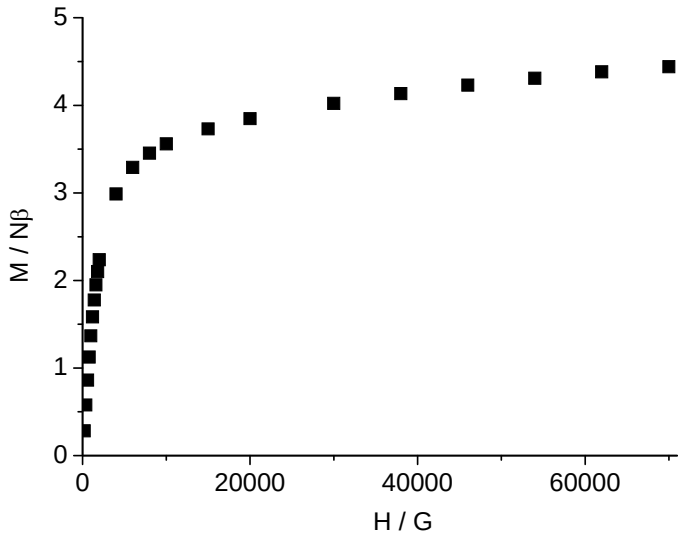

Fig. S7. Plot of M versus H for **2** at 2 K.

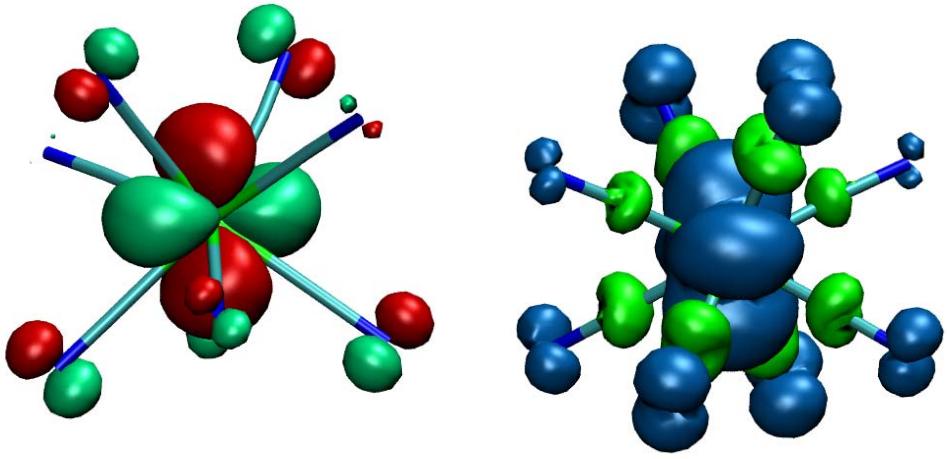

(a) (b)

Fig. S8. (a) Natural molecular magnetic orbital and (b) spin density of the $[Mo(CN)_8]^{3-}$ precursor with a Mo d_{x2-y2} type magnetic orbital, derived from B3LYP DFT calculations performed with Gaussian 09. The basis set for all atoms is LANL2DZ. For **1**, NBO analysis shows that spin density is 0.8927 on Mo, 0.01369 and 0.01849 on bridging N atoms, and 0.03747 – 0.07293 on the other free N atoms. For **2**, NBO analysis shows that spin density is 0.91842 on Mo, 0.02021 and 0.02236 on bridging N atoms, and 0.02928 – 0.08814 on the other free N atoms.

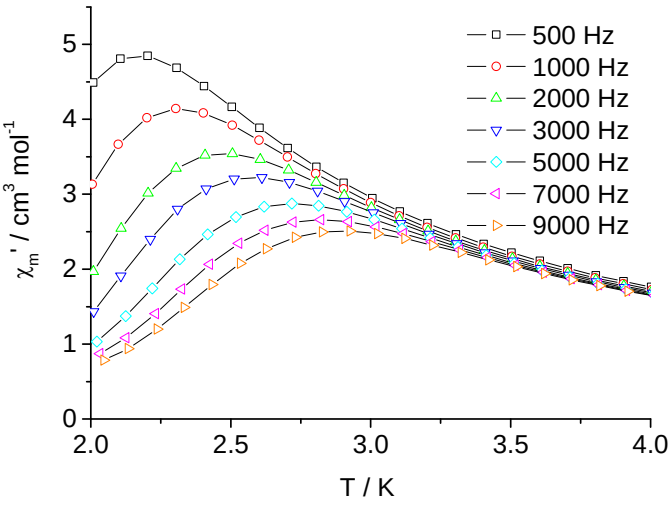

Fig. S9. In-phase ac susceptibility data (χ_m') versus temperature plot for **1** at the indicated frequencies.

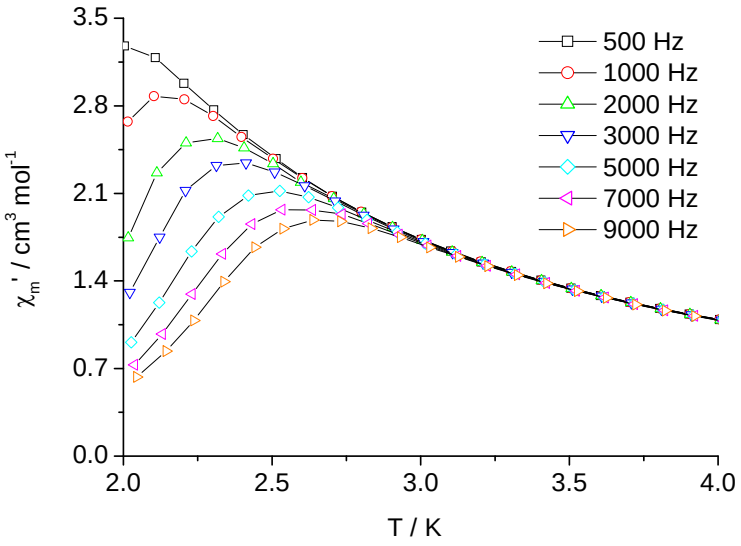

(a)

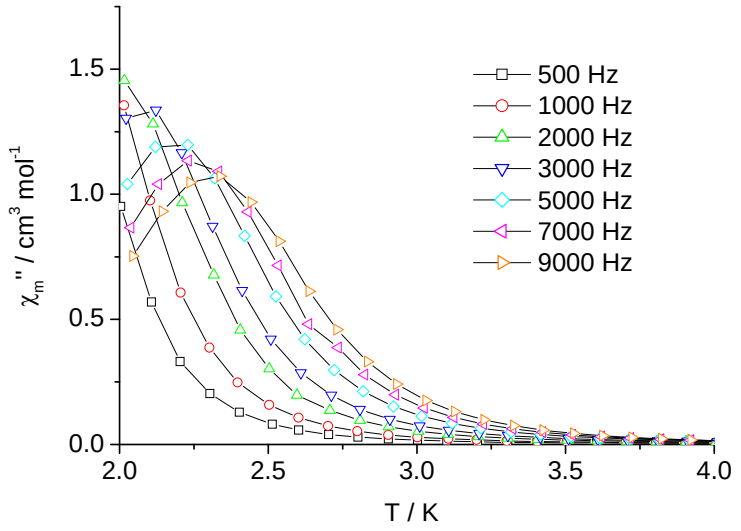

(b)

Fig. S10. Plots of χ_m' and χ_m" versus *T* plot for **2** at the indicated frequencies.

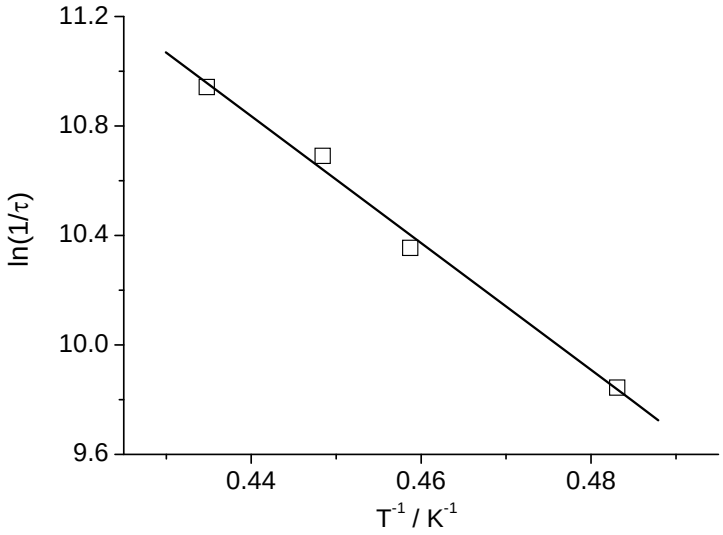

Fig. S11. Arrhenius plot for **2**. The solid line stands for the least-squares fit of the maxima in χ_m" to the Arrhenius equation

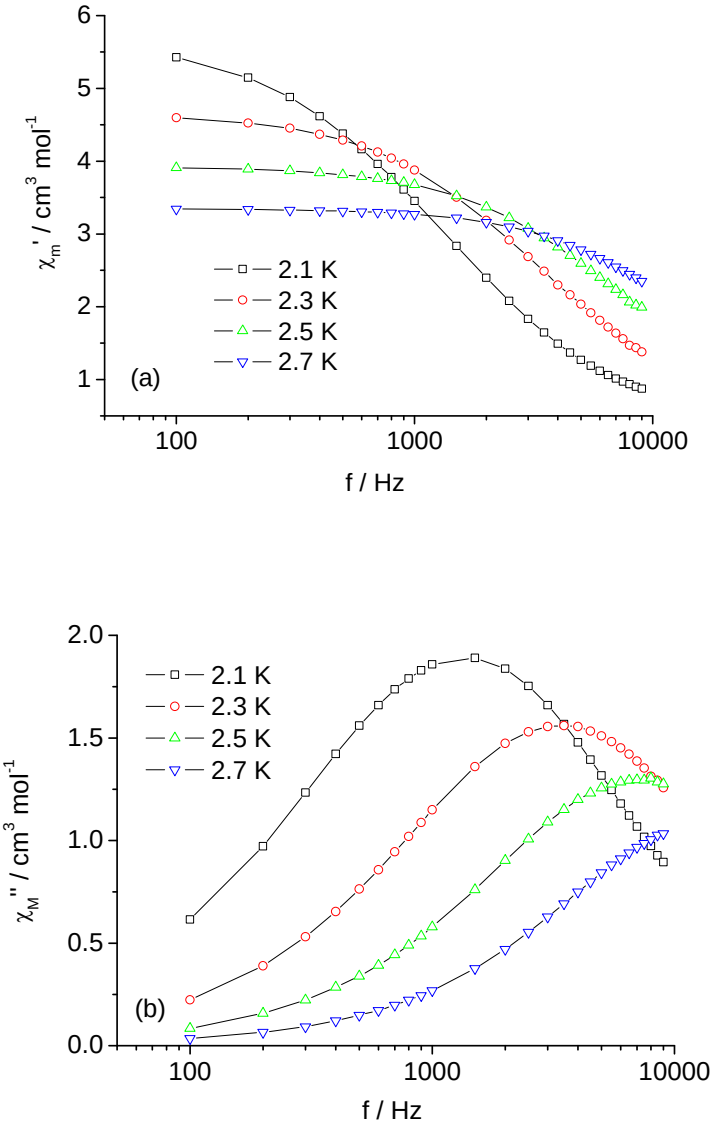

Fig. S12. Frequency dependence of ac susceptibilities for **1**.

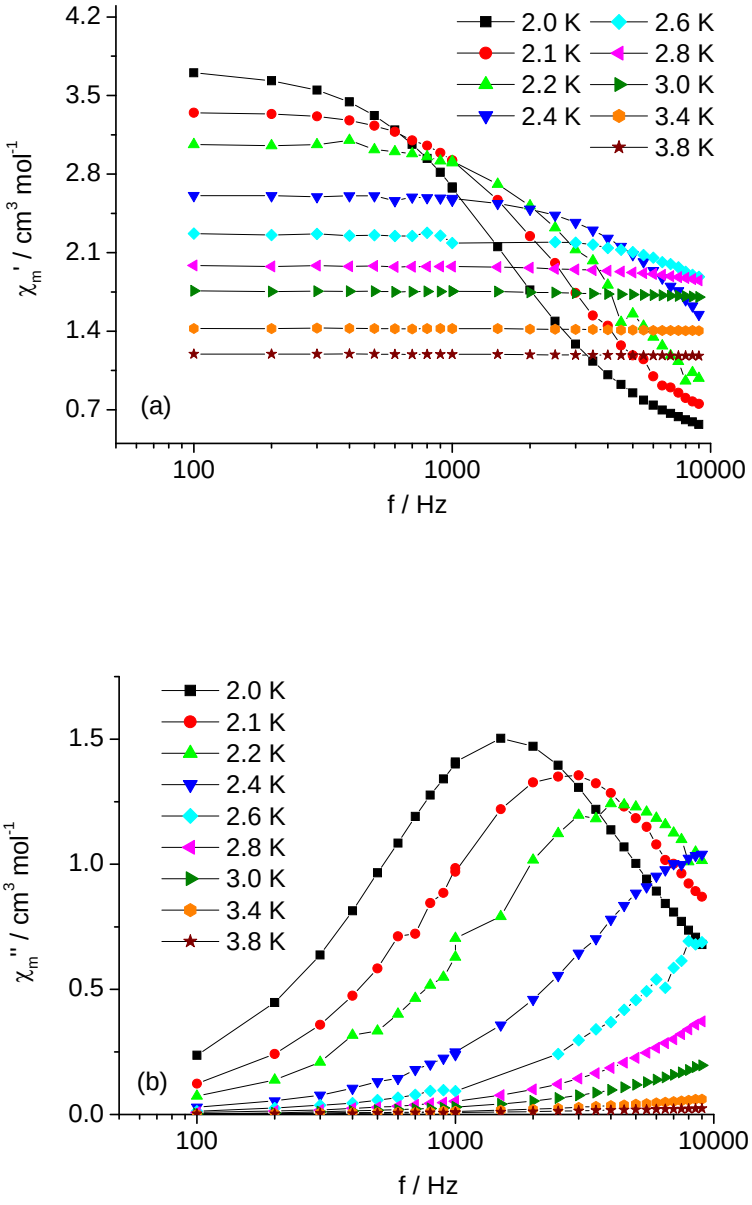

Fig. S13. Frequency dependence of ac susceptibilities for **2**.

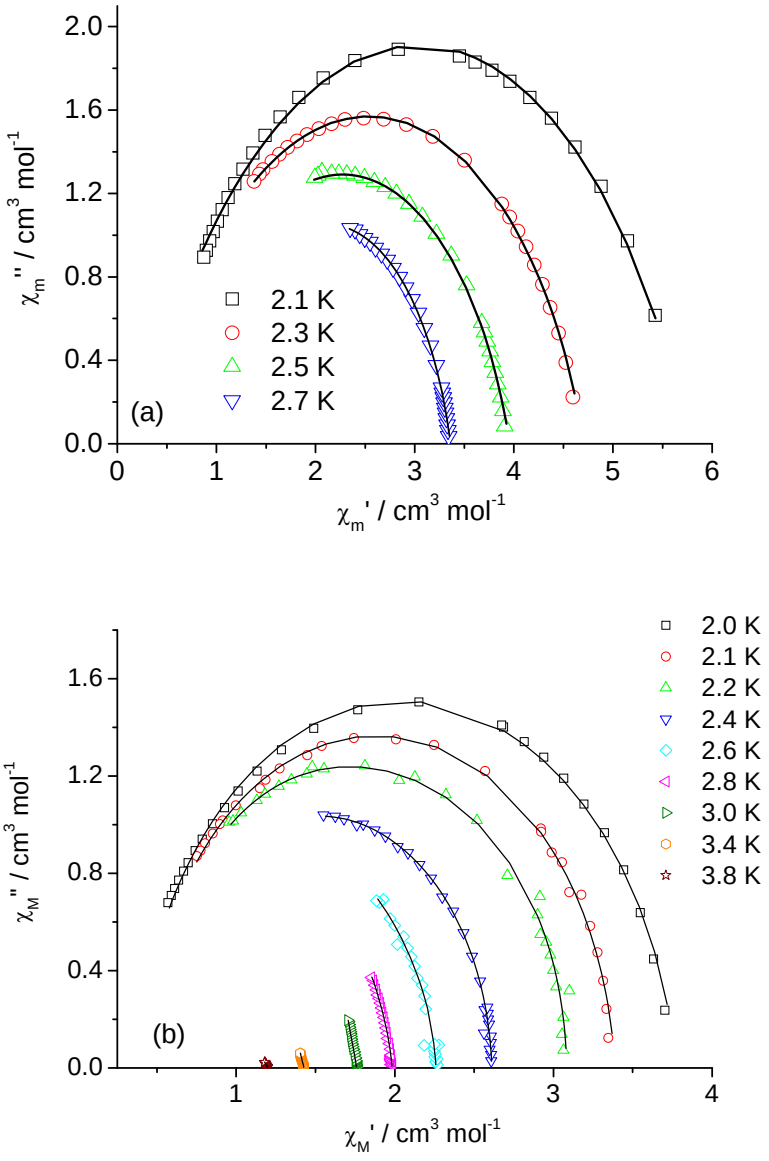

Fig. S14. Cole-Cole plots and fitted results with a generalized Debye model for (a) **1** and (b) **2** at the indicated temperatures

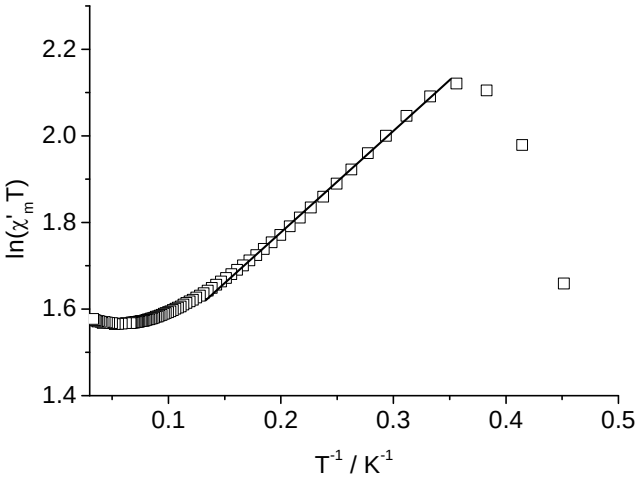

Fig. S15. Semilog plot of χ_m'T versus 1/T for **1**. The solid line represents the fit using the equation given in the text.

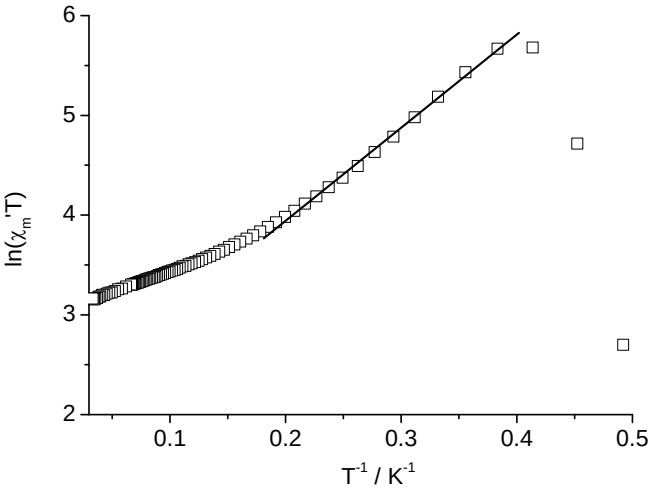

Fig. S16. Semilog plot of χ_m'T versus 1/T for **2**. The solid line represents the fit using the equation given in the text.